RETRIEVING THE PROFILE OF ATTENUTATION FACTOR FROM DATA OF ONE−ANGLE LIDAR SENSING

V.A. Kovalev, E.E. Rybakov, and V.M. Ignatenko

A.I. Voeikov Main Geophysical Observatory, Leningrad
Received February 4, 1991

Algorithms are described for retrieving the profile of attenuation factor (or transmittance) along the beampath from lidar returns. The inversion procedure preassumes the validity of single−scattering approximation and the power−law dependence of backscattering on the coefficient attenuation. Two different algorithms of retrieval of the profile of attenuation coefficient are discussed. Examples of experimental data are given.

To retrieve the profile of attenuation coefficient from data of lidar sensing the well−known equation of laser sensing is usually used in its single−scattering approximation

$$P(z) = A \cdot r_\pi(z) \cdot z^{-2} \cdot \exp\left(-2 \int_0^z \mu(z') dz' \right). \qquad (1)$$

where $P(z)$ is the backscattered signal from a distance z from the lidar, $r_\pi(z)$ is the coefficient of backscattering, $\mu(z)$ is the attenuation coefficient, and A is the lidar constant.

When using Eq. (1) to retrieve the profile of attenuation coefficient along the beampath one needs:

a) to retrieve or prescribe *a priori* the relation between the total scattering coefficient and the backscattering one and

b) to determine the constant A which may be done, for example, if the characteristics of the sensed medium are known within the fixed section of the sensed path. Most often such characteristics are either determined or *a priori* prescribed at the ends of the sensed path, i.e., the constant A is determined using the boundary conditions.

The relation between the backscattering coefficient r_π, and the total scattering coefficient r is usually written in the form

$$r_\pi = C \cdot r^K , \qquad (2)$$

where C and K are constants. For a purely scattering medium ($r(z) = \mu(z)$) Eq. (1) may then be rewritten in the form convenient for practical use

$$S(z) = B \cdot [\mu(z)]^K \cdot \exp\left(-2 \int_{z_0}^z l(z') dz' \right). \qquad (3)$$

Here the function $S(z) = P(z) \cdot z^2$ called the S−function, is the backscattered signal corrected for squared distance. The parameter $B = A \cdot C \cdot T_0^2$ may be called the constant of the S−function, to differ from the constant A in Eq. (1); T_0 is the atmospheric transmittance within the near field for the lidar proximity zone $[0, z_0]$.

In this approximation the parameter C in Eq. (2) is one of the factors in the constant of the S−function, which is determined with the chosen boundary conditions. The key moment in practical use of Eq. (3) is then the choice of the numerical value of the parameter K. Many studies

demonstrate that within a wide range of turbidities varying from weak to dense hazes, the parameter K is on the average close to 0.7. However, large deviations from this value are often observed.[1−5] For this reason in experimental studies when the parameter K has to be approximately prescribed, it is chosen to be equal to unity for simplicity.[6−10]

As for assigning the boundary conditions, those processing techniques which employ rather weak *a priori* assumptions find the widest use. Among them are, for example, the techniques of multiangle sensing, which have lately found an extensive use.[7,9−15] Additional data available (as compared to the one−angle techniques) make it possible to check the correctness of the initial assumptions thereby significantly improving the reliability of measurements. Unfortunately, these techniques are applicable mainly to rather a stable atmosphere. The techniques of one−angle sensing are simpler for realization, more operative, and may be used under highly complex and rapidly varying optical conditions. However, the need to use some sort of an *a priori* information to retrieve the constant B of the S−function seriously impeded the measurement process.[16−18] As has been mentioned above, this problem can be solved in a simplest way in the case in which the characteristics of optical turbidity of the atmosphere are known within the fixed section of the beampath during the experiment.

Unfortunately, the application with this aim some parallel measurements of the optical characteristics of the atmosphere with the help of the independent instruments is rather difficult. In practice, in sensing the atmosphere along the slant paths, it is necessary either to use measurements with the same lidar along auxiliary paths (usually horizontal[7,9,19]) or to prescribe speculatively the attenuation coefficient within a fixed section of the sensed path. In the latter case some assumptions on the turbidity along the path are most often employed (for example, the assumption that there exist homogeneously turbid local sections along the path,[20] or sections with purely molecular scattering,[21,22] and so on). Introduction of such an approach to the determination of the constant B has stimulated a lively discussion concerning the problem of choosing this or that reference section of the path.[23−27] The analysis demonstrated that the option suggested by Klett, according to which this reference point is chosen on the far section or on the very end of the path,[23] is preferable from the view point of the solution stability at least for the turbid sensed atmosphere with comparatively large optical thicknesses.

As far back as 1980 one of the authors of the present study suggested to determine the constant of the S−function in one−angle sensing of the inhomogeneous atmosphere from

the shape of the received backscattered signal.[20] Modifying it we concluded that such an approach should be further extended. The idea is to start processing of returns in lidar sensing of the aerosol atmosphere from the identification of the actual optical situation. Such an identification may be based, for example, on analyzing the shape of the received backscattered signal.

Now we restrict ourselves to the processing techniques applicable to such optical situations when, within the entire sensed path $[z_0, z_m]$ (z_m is the sensing range) the S−functions vary by no more than 12–15 dB, and the relationship $z_m/z_0 \geq D$ holds. The parameter D depends on the characteristics of the lidar used, e.g., for the Elektronika−06R lidar[28] we have $D = 3$. According to the data found in the references the Klett technique[20] is the most appropriate for such optical situations. However, we consider that in order to determine the constant B of the S−function it is more appropriate to use the integral characteristics of the atmospheric turbidity along the beampath such as the total double transmittance $T_m^2(z_0, z_m)$ of the entire sensed path from z_0 to z_m instead of the local characteristics. Such an approach simultaneously with the technique of asymptotic signal[29] makes it possible not only to ensure the stability of the obtained solution, but also needs no absolute calibration of the lidar (for example, in contrast to the technique described in Ref. 30), which significantly simplifies the process of measurements. The sought−after profiles of transmittance $T(z_0, z_m)$ and of the attenuation coefficient $\mu(z)$ for $z < z_m$ will have the following form:

$$T(z_0, z) = \left[\frac{J_2}{J_m} + \frac{J_1}{J_m} \cdot T_m^{2/K}\right]^{K/2} ; \tag{4}$$

$$l(z) = \frac{[S(z)]^{1/K}}{\dfrac{2}{K}\left[\dfrac{J_m}{1 - T_m^{2/K}} - J_1\right]} . \tag{5}$$

Here $J_1 = \int\limits_{z_0}^{z}[S(z')]^{1/K}\mathrm{d}z'$; $J_2 = \int\limits_{z}^{z_m}[S(z')]^{1/K}\mathrm{d}z'$; $J_m = J_1 + J_2$; $T_m = T_m(z_0, z_m)$.

Relations (4) and (5) for $k = 1$ take the form

$$T(z_0, z) = \left[\frac{J_2}{J_m} + \frac{J_1}{J_m} \cdot T_m^2\right]^{1/2} ; \tag{6}$$

$$\mu(z) = \frac{S(z)}{2\left[\dfrac{J_m}{1 - T_m^2} - J_1\right]} . \tag{7}$$

To perform calculations based on Eqs. (6) and (7) the parameter T_m^2 should be preliminary estimated. In the case of low visibility when the total optical thickness τ_m of the sensed layer $[(z_0, z_m)]$ satisfies the condition

$$\tau_m \gtrsim 1.5 , \tag{8}$$

the value T_m^2 may be estimated from the formula

$$T_m^2 \approx \frac{S(z_m)}{S(z_0)} . \tag{9}$$

The criterion of satisfying condition (8) may generally be taken in the form

Ошибка! . $\tag{10}$

Note that certain additional criteria of satisfying Eq. (8) were used in practice. This allowed us to identify such specific situations as, for example, surface haze, elevated fog, and so on.

Relations (6)–(10) are applicable if the condition $K \approx \mathrm{const}$ holds for the entire sensed path. However, in the case in which the two−layered media are sensed (e.g., subcloud haze−cloud) in which the scattering phase function sharply changes at the interface between the two media, and a strong spike in the backscattered signal reflected from the cloud is recorded at the end of the path, employing relations (6)–(10) may result in significant systematic errors in the measured parameters. This situation forces us to sort out such cases and to apply different processing algorithms to them. As for the situation described above a special algorithm was constructed, which was based on dividing the entire sensed path into two sections. The interface between the two media was determined by the position of the spike in the reflected signal, and different values of the coefficient K were chosen for each section of the path.

Let us consider the stages of this process. The choice of the parameter K is based on the results of Ref. 1, in which numerous theoretical and experimental data were analyzed to relate the total scattering coefficient and the backscattering one. This analysis demonstrated that although the concrete values C and K differ significantly, depending on the conditions of the experiment, the dependence of these parameters on the measured values of μ is predominant. Based on the data of this study the authors of Ref. 1 proposed a certain averaged dependence relating the total scattering coefficient and backscattering one within the range of variation of the turbidity from 10^{-2} to 20–30 km^{-1}. While the attenuation coefficient remains within the limits 2–3 km^{-1}, the obtained dependence has a quite sharp break and the corresponding dependence of r_π on μ may be represented in the form

$$r_\pi = \begin{cases} C_1 \cdot \mu^{K_1} \text{ for } \mu < \mu_b , \\ C_2 \cdot \mu^{K_2} \text{ for } \mu > \mu_b , \end{cases} \tag{11}$$

where the boundary value of μ_b lies within 2–3 km^{-1} and the values K_1 and K_2 − within 0.6–0.7 and 1.3–1.5, respectively. Therefore, when sensing the two−layered media of the haze−cloud type it is advisable to use the value $K = K_1$ in the haze section of the path and $K = K_2$ in its cloud section. Then the formula relating $\mu(z)$ to $r_\pi(z)$ along the path is written in the form

$$r_\pi(z) = \begin{cases} C_1 |\mu(z)|^{K_1} \text{ for } z < z_b , \\ C_2 |\mu(z)|^{K_2} \text{ for } z \geq z_b , \end{cases} \tag{12}$$

where z_b specifies the position of the interface between the two media. If may be found by analyzing the shape of the reflected signal.

As shown earlier in Ref. 20, the constant of the S−function may be found from the relation of the form

$$B = \frac{S(z_i)}{\mu(z_i)} + 2\int\limits_{z_0}^{z_i} S(z)\mathrm{d}z , \tag{13}$$

which is true for $K = 1$. Here z_i determines the distance to the point i along the path at which the attenuation coefficient $\mu(z_i)$ is assumed either to be well known or determined in other way.

Choosing $z_i = z_b$ and taking into account that in our case $K = K_1$ in the subcloud layer, Eq. (13) may be written in the form

$$B = \left\{ \frac{[S(z_b)]^{1/K_1}}{\mu(z_b)} + \frac{2}{K_1}\int_{z_0}^{z_b}[S(z')]^{1/K_1}\mathrm{d}z' \right\}^{K_1}. \tag{14}$$

It is follows from Eq. (14) that to estimate B we must know $\mu(z_b)$. To find the latter we use the profile of the signal backscattered from the cloud, i.e., from distances larger than z_b. For arbitrary z_i satisfying the condition $z_b < z_j < z_{m_2}$ (z_{m_2} is the maximum sensing range within the cloud) it may be written in accordance with Eq. (5)

$$(\mu(z_j) = \frac{[S(z_j)]^{1/K_2}}{\frac{2}{K_2}\left[\dfrac{J_{m_2}}{1 - T_{m_2}^{2/K_2}} - \displaystyle\int_{z_b}^{z_j}[S(z')]^{1/K_2}\mathrm{d}z' \right]}. \tag{15}$$

We obtain for $z_j \to z_b$:

$$\mu(z_b) = \frac{K_2[S(z_b)]^{1/K_2} \cdot [1 - T_{m_2}^{2/K_2}]}{2J_{m_2}}, \tag{16}$$

where $J_{m_2} = \displaystyle\int_{z_b}^{z_{m_2}}[S(z')]^{1/K_2}\mathrm{d}z'$ and T_{m_2} is the transmittance of the layer $[z_b, z_{m_2}]$

$$T_{m_2} = \exp[-\overline{\mu}_{\mathrm{cl}}(z_{m_2} - z_b)]. \tag{17}$$

When estimating T_{m_2} the attenuation factor within the cloud μ_{cl} may be either assigned *a priori* or estimated in any way, e.g., from the steepness of the signal slope within the cloud by the method of logarithmic derivative. It should be noted that if the problem is to retrieve the profile of $\mu(z)$ in the subcloud layer or in the initial part of the cloud, the requirements for the accuracy of estimating T_{m_2} are not stringent. At the same time when retrieving the profile of $\mu(z)$ in the cloud depth, and particularly for z close to z_{m_2}, the measurement errors caused by the errors in estimating $\overline{\mu}_{\mathrm{cl}}$, or by the effects of multiple scattering, and so on, sharply increase; for this reason it is undesirable to use Eqs. (14) and (16) to retrieve the optical characteristics of clouds by themselves.

The algorithms considered above were developed and tested during the extensive cycle of the experimental investigations. At the first stage the possibilities of using

algorithms (6)–(10) were tested. This study was performed at the end of 1987 in Voeikovo, and in fall of 1988 in Dubna of the Moscow region with the help of an Elektronika–03 lidar equipped with a digital recording system. These studies were accompanied by reference measurements of the transparency with the help of transmisson meters operating along the horizontal paths in Voeikovo and along the slant paths (from a 30–m tower) in Dubna. Results of these tests have been published in Refs. 31 and 32.

Comparing the lidar data with reference measurements demonstrated that the above processing algorithm provides in general a good agreement with data of reference instruments, including those from slant paths under conditions of low visibility, and that this algorithm is promising for retrieving the transparency profiles for a wide range of the studied meteorological conditions.

Algorithms for processing the backscattered signals, in which the path is divided into two sections and different values of the parameter K are used for each of these sections, were tested at the Ul'yanovsk airport in April, 1989 with the help of an Elektronika–06R lidar. The vertical profiles of the attenuation factor obtained in such a way were used to calculate the altitude of visual reference (AVR) with the lights of the runway. The technique of these calculations may be found in Refs. 33–35. Simultaneously the AVR was visually determined from onboard the descending aircraft. These comparisons were accompanied by measurements of the cloud base height (CBH) and the meteorological visibility range (MVR) with the standart meteorological equipment of the airport.

Figure 1 shows the typical shape of the reflected signal (of the S–function) $S(h)$, obtained in sensing the two–layered haze–cloud medium. The spike in the signal at 200 m is caused by SC cloudiness with the 200 m CBH according to the standard cloud base height meter; the MVR near the ground was 5–7 km. Signals obtained under such conditions have low amplitude within the near field, high amplitude reflected from the cloud, and almost continuously increased $S(h)$ along the entire lower section of the beampath up to the cloud base hight. The dashed line in Fig. 1 denotes the range h_b corresponding to the chosen altitude z_b ($h_b = z_b \cdot \sin\varphi$, where φ is the observation angle).
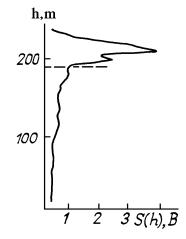

FIG. 1. *Shape of the lidar return S(h) from the cloudy atmosphere on April 15, 1989 at 11.20 LT at an observation angle of 13.6°.*
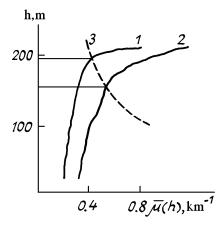
FIG. 2. Vertical profiles of the attenuation factor

$$\overline{\mu}(h) = -\frac{1}{h}\int\limits_0^h \mu(h')\mathrm{d}h' \text{ corresponding to signal } S(h) \text{ shown}$$

in Fig. 1, and to different processing algorithms (3 denotes the boundary curve for determining the AVR).

Figure 2 shows the vertical profile of the average attenuation factor $\overline{\mu}(h)$, retrieved from the signal $S(h)$ with a constant coefficient K assigned over the entire sensed path (curve 1), and the corresponding profile obtained using the algorithm for the two–layered atmosphere (curve 2). The sought–after value of the AVR is found as the point of intersection of the profile of the average attenuation factor $\overline{\mu}(h)$ and the preliminarily calculated boundary curve 3, determining the limiting values of the attenuation factor for which the runway lights disappear under the given observational conditions.[34,35] As can be seen from the figure the difference between the values of the AVR obtained from both profiles is about 40 m, in addition, the profile represented by curve 1 overestimates the AVR.

Figure 3 shows the temporal behavior of the AVR from the data of lidar sensing of a cloudy atmosphere for both the one–layered (curve 1) and the two–layered (curve 2) atmospheres. Triangles show the altitudes of visual reference with runway lights, according to visual observations from onboard the descending aircraft. A good agreement between these observations and results of processing the lidar returns using the algorithm of the two–layered atmosphere testifies, first, the feasibility of its use when the strong spike from the cloud layer can be seen in the signal at the end of the sensed path, and, second, the need for preliminary identification of the meteorological situation, in which this signal is recorded.
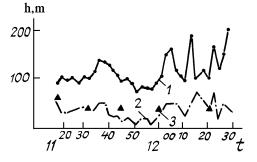

FIG. 3. Temporal behavior of the AVR from lidar sensing data and from visual observations performed from onboard the descending aircraft on April 15, 1989. The CBH is 180–220 m.

REFERENCES

1. V.A. Kovalev, G.N. Baldenkov, and V.I. Kozintsev, Isv. Akad. Nauk SSSR, Ser. FAO **23**, No. 6, 611–615 (1987).
2. J.D. Klett, Appl. Opt. 24, No. 11, 1638–1643 (1985).
3. J.M. Mulders, Appl. Opt. **23**, No. 17, 2855–2856 (1984).
4. H.G. Hughes, J.A. Ferguson, and D.H. Stephens, Appl. Opt. **24**, No. 11, 1609–1613 (1985).
5. K. Parameswaran, K.O. Rose, and B.V.K. Mirthy, in: *Abstracts of Reports of the Fifteenth International Laser Radar Conference*, Tomsk (1990), Vol 1, pp. 180–184.
6. W. Carnuth and R. Reiter, Appl. Opt. **25**, No. 17, 2899–2907 (1986).
7. G.J. Kunz, Appl. Opt. **22**, No. 13, 1955–1957 (1983).
8. J. Sasano, Appl. Opt. **27**, No. 13, 2640–2641 (1988).
9. G. Leeuw, in: *Abstracts of Reports at Opt. and Millim. Wave Propag. Scatter. Atm.,* May 27–30, 1986, pp. 101–104.
10. V.A. Kovalev, V.M. Ignatenko, et al., *Abstracts of Reports at the Seventh All–Union Conference on Laser and Acoustic Sensing of the Atmosphere*, Tomsk (1984), Vol. 1, pp. 61–63.
11. V.A. Lyadzhin, B.T. Tashenov, and T.P. Toropova, Atm. Opt. **3**, No. 3, 277–284 (1990).
12. J.A. Reagan, M.V. Arte, et al., Aerosol Science and Technol., No. 8, 215–226 (1988).
13. J.D. Spinhirne, J.A. Reagan, and B.M. Herman, Journ. Appl. Meteorol. **19**, 426–438 (1980).
14. J.L. Gaumet and A. Petitpa, Journ. Appl. Meteorol. **21**, No. 5, 683–694 (1982).
15. J. Kolev, O. Parvanov, et al., *Abstracts of Reports at the Fifteenth International Laser Radar Conference,* Tomsk, (1990), Vol. 1, pp. 244–249.
16. V.E. Zuev, S.I. Kavkyanov, and G.M. Krekov, Izv. Akad. Nauk SSSR, Ser. FAO **19**, No. 3, 255–266 (1983).
17. S.I. Kavkyanov and G.M. Krekov, in: *Methods for Laser Sensing,* M.V. Kabanov (Nauka, Novosibirsk, 1980), pp. 3–39.
18. G.M. Krekov, S.I. Kavkyanov, and M.M. Krekova, *Interpreting the Signals of Optical Sensing of the Atmosphere* (Nauka, Novosibirsk, 1987), 172 pp.
19. G.M. Krekov and I.V. Samokhvalov, in: *Absracts at Reports of the Third All–Union Symposium on Laser Sounding of the Atmosphere,* Tomsk, 1974, pp. 45–46.
20. V.A. Kovalev and A.G. Kuz'min, Trudy GGO (MGO Proceedings) **419**, 100–101 (1980).
21. S. Elouragini, L. Menenger, et al., in: *Abstracts of Reports at the Fifteenth International Laser Radar Conference*, Tomsk (1990), Vol. 1, pp. 359–362.
22. U.N. Singh, A. Notari, et al., ibid., 318–319.
23. J.D. Klett, Appl. Opt. **20**, No. 2, 211–220 (1981).
24. L.R. Bissonette, ibid. **25**, No. 13, 2122–2125 (1986).
25. J.A. Ferguson and D.H. Stephens, ibid. **22**, No. 23, 3673–3675 (1983).
26. D.C. Knauss, ibid. **21**, No. 23, 4194 (1982).
27. S.R. Pal, A.G. Gunningham, and A.J. Garswell, in: *Abstracts of Reports at the Fifteenth International Laser Radar Conference*, Tomsk (1990), Vol. 1, pp. 152–153.
28. G.N. Baldenkov, E.E. Mozharov, et al., ibid., Tomsk (1990) Vol. 1, pp. 380–381.
29. V.A. Kovalev, Trudy GGO (MGO Proc.) **312**, 128–133 (1973).
30. E.V. Browell, S. Ismail, and S.T. Shipley, Appl. Opt. **24**, No. 17, 2827–2836 (1985).
31. Ye.E. Mozharov, G.N. Baldenkov, et al., in: *Abstracts of Reports of the Tenth All–Union Conference on Laser and Acoustic Sensing of the Atmosphere*, Tomsk (1989), Vol. 1, pp. 58–62.

32. V.A. Kovalev, E.E. Rybakov, and E.E. Mozharov, in: *Abstract of Reports at Fifteenth Laser Radar Conference,* Tomsk (1990), Vol. 1, pp. 282−283.
33. M.Ya. Ratsimor, *Slant Visibility* (Gidrometeoizdat, Leningrad, 1987), 136 pp.
34. V.A. Kovalev, *Visibility in the Atmosphere and its Determination* (Gidrometeoizdat, Leningrad, 1988), 216 pp.
35. E.E. Rybakov, Trudy GGO (MGO Proc.) **519**, 144−150 (1988).